Model Predictions of Latitude-Dependent Ozone Depletion Due to Supersonic Transport Operations

W.J. Borucki,* R.C. Whitten,* V.R. Watson,† and H.T. Woodward*
NASA Ames Research Center, Moffett Field, Calif
C.A. Riegel‡ and L.A. Capone§
San Jose State University, San Jose, Calif.
and
T. Becker¶
Informatics, Inc., Palo Alto, Calif.

Results are presented from a two-dimensional model of the stratosphere that simulates the seasonal movement of ozone by both wind and eddy transport, and contains all the chemistry known to be important. The calculated reductions in ozone due to NO_2 injection from a fleet of supersonic transports are compared with the zonally averaged results of a three-dimensional model for a similar episode of injection. The agreement is good in the northern hemisphere, but is not as good in the southern hemisphere. Both sets of calculations show a strong corridor effect in that the predicted ozone depletions are largest to the north of the flight corridor for aircraft operating in the northern hemisphere.

Introduction

CALCULATIONS by previous workers such as Johnston,[1] McElroy et al.,[2] Crutzen,[3] and Whitten et al.[4] have shown that the operation of aerospace vehicles in the Earth's stratosphere can be expected to deplete the Earth's ozone layer. The majority of these calculations are based on one-dimensional models that do not simulate the horizontal movement of ozone and other tracers by winds. Hence, the models cannot be used to calculate the latitude dependence of the ozone depletion.

Recently, preliminary calculations have become available from models[5-8] that do simulate the transport of ozone by winds. However, because these models are still in the developmental stage, each model as yet has not included some important factor, such as seasonal transport, nitric-acid chemistry, or the simultaneous solution of the odd-oxygen/odd-nitrogen chemical systems.

This paper presents results from a two-dimensional model that simulates seasonal transport of ozone by winds and contains all the chemistry presently known to be important. Comparisons of model predictions with experimental measurements for the spread of a radioactive tracer from nuclear tests are presented as well as the model predictions for the perturbations in the stratosphere caused by aerospace vehicles.

The Model

The model is based upon the governing equations for trace constituents

$$(\partial n_i/\partial t) + \nabla \cdot n_i v + \Phi_i = Q_i \qquad (1)$$

$$\underset{\sim}{\Phi}_i = -\underset{\approx}{K}_e \left[\underset{\sim}{\nabla} n_i + \left(\frac{1}{H} + \frac{1}{T}\frac{dT}{dz} \right) n_i \hat{e}_z \right] \qquad (2)$$

in which n_i and $\underset{\sim}{\Phi}_\theta$ are the concentration and flux, respectively, of the i^{th} constituent, Q_i is the respective chemical production and loss rate term, H and T are the atmospheric scale height and temperature, $\hat{e}_z$ is a vertical unit vector, v is the bulk velocity of the atmosphere, and $\underset{\approx}{K}_e$ is the eddy diffusivity tensor.

The chemical rate equations are solved using an implicit technique. Omitting the transport term from Eq. (1) yields the finite difference form

$$(n_i^{j+1} - n_i^j)/\Delta t = Q_i^{j+1} \qquad (3)$$

which can be linearized by taking the first term in a Taylor series expansion of Q_i^{j+1} about Q_i^j

$$\frac{n_i^{j+1} - n_i^j}{\Delta t} = Q_i^j + \sum_k \frac{\partial Q_i^j}{\partial n_k} \left(n_k^{j+1} - n_k^j \right) \qquad (4)$$

The members of the set of mass conservation equations are coupled and require solution by matrix methods. With the implicit method, large time steps can be taken even though the equations are very stiff.

The transport computations are time-split into those for vertical and horizontal advection and diffusion. Solutions for the transport processes are obtained from a mass conserving, forward time, space-centered finite difference formulation of the equations. An implicit formulation is used for the horizontal diffusion and an explicit formulation is used for all other transport processes.

Spherical geometry is employed in Eqs. (1) and (2) with the horizontal coordinate extending along a meridian from 80°S to 80°N in 5° intervals and the vertical coordinate extending from the ground to 60 km in 2.5-km intervals (Fig. 1). End boundaries are taken at 80°S and 80°N because meridional fluxes are expected to be small at these latitudes. The end boundary conditions are taken to be zero flux of all constituents across the vertical boundaries. The upper boundary conditions are given by setting the vertical flux equal to zero for all species. The lower boundary condition for all species

Presented as Paper 76-176 at the AIAA 14th Aeorspace Sciences Meeting, Washington, D. C., Jan 26-28, 1976; submitted Feb. 20, 1976; revision received Sept. 29, 1976.

Index category: Atmospheric, Space, and Oceanographic Sciences.

*Research Scientist, Theoretical and Planetary Studies Branch.

†Research Scientist, Theoretical and Planetary Studies Branch. Member AIAA.

‡Professor of Meteorology.

§Meteorologist.

¶Programmer.

Table 1 Reaction rate coefficients[a]

Number	Process	Reaction rate coefficient	Reference
1	$O + O_3 \rightarrow 2\ O_2$	$1.9\times10^{-11}\ \exp(-2300/T)$	11
2	$O + O_2 + M \rightarrow O_3 + M$	$1.1\times10^{-34}\ \exp(510/T)$	12
3	$NO_2 + O \rightarrow NO + O_2$	9.1×10^{-12}	13
4	$NO + O_3 \rightarrow NO_2 + O_2$	$9.0\times10^{-13}\ \exp(-1200/T)$	14
5	$NO_3 + NO \rightarrow 2\ NO_2$	2.0×10^{-11}	12
6	$O_3 + NO_2 \rightarrow NO_3 + O_2$	$6.3\times10^{-12}\ \exp(-3500/T)$	12
7	$O(^1D) + M \rightarrow O + M$	5.4×10^{-11}	15
8	$O + OH \rightarrow H + O_2$	4.2×10^{-11}	12
9	$O_3 + H \rightarrow OH + O_2$	2.6×10^{-11}	12
10	$NO + O + M \rightarrow NO_2 + M$	$3.0\times10^{-33}\ \exp(940/T)$	16
11	$NO_2 + NO_3 + M \rightarrow N_2O_5 + M$		17[b]
12	$O(^1D) + H_2O \rightarrow 2\ OH$	3.5×10^{-10}	14
13	$O_3 + HO_2 \rightarrow OH + 2\ O_2$	$1.0\times10^{-13}\ \exp(-1250/T)$	12
14	$O + HO_2 \rightarrow OH + O_2$	$8.0\times10^{-11}\ \exp(-550/T)$	12
15	$NO_2 + OH + M \rightarrow HNO_3 + M$		17[b]
16	$OH + HNO_3 \rightarrow H_2O + NO_3$	$6.0\times10^{-13}\ \exp(-400/T)$	12
17	$O + O + M \rightarrow O_2 + M$	1.0×10^{-32}	12
18	$OH + HO_2 \rightarrow H_2O + O_2$	6.0×10^{-11}	12
19	$OH + CO \rightarrow H + CO_2$	1.36×10^{-13}	12
20	$H + O_2 + M \rightarrow HO_2 + M$	$6.7\times10^{-33}\ \exp(290/T)$	12
21	$O + HNO_3 \rightarrow OH + NO_3$	1.5×10^{-14}	12
22	$OH + O_3 \rightarrow HO_2 + O_2$	$1.6\times10^{-12}\ \exp(-1000/T)$	11
23	$NO + HO_2 \rightarrow NO_2 + OH$	2.0×10^{-13}	12
24	$NO_2 + O + M \rightarrow NO_3 + M$		17[b]
25	$N_2O_5 + M \rightarrow NO_2 + NO_3 + M$		17[b]
26	$H + OH + M \rightarrow H_2O + M$	$6.1\times10^{-26}\ T^{-1/2}$	12
27	$N + O_3 \rightarrow NO + O_2$	5.7×10^{-13}	12
28	$N + NO \rightarrow N_2 + O$	2.7×10^{-11}	12
29	$N + O_2 \rightarrow NO + O$	$1.1\times10^{-14}\ T\ \exp(-3150/T)$	12
30	$N + OH \rightarrow NO + H$	5.7×10^{-11}	12
31	$NO + OH + M \rightarrow HNO_2 + M$	$2.2\times10^{-32}\ \exp(1100/T)$	12
32	$NO_2 + HO_2 \rightarrow HNO_2 + O_2$	3.0×10^{-14}	12
33	$OH + HNO_2 \rightarrow H_2O + NO_2$	1.3×10^{-13}	12
34	$O(^1D) + N_2 + M \rightarrow N_2O + M$	2.8×10^{-36}	12
35	$O(^1D) + N_2O \rightarrow N_2 + O_2$	1.1×10^{-10}	12
36	$O(^1D) + N_2O \rightarrow 2\ NO$	1.1×10^{-10}	12
37	$O + HNO_2 \rightarrow OH + NO_2$	1.5×10^{-14}	12
38	$OH + OH + M \rightarrow H_2O_2 + M$	$2.5\times10^{-33}\ \exp(2550/T)$	12
39	$OH + H_2O_2 \rightarrow H_2O + HO_2$	$1.7\times10^{-11}\ \exp(-910/T)$	12
40	$HO_2 + HO_2 \rightarrow H_2O_2 + O_2$	$3.0\times10^{-11}\ \exp(-500/T)$	12
41	$O + H_2O_2 \rightarrow OH + HO_2$	$1.1\times10^{-12}\ \exp(-2125/T)$	18, 19[c]
42	$O + H_2O_2 \rightarrow H_2O + O_2$	$1.6\times10^{-12}\ \exp(-2125/T)$	18, 19[c]
43	$HCl + OH \rightarrow H_2O + Cl$	$2.8\times10^{-12}\ \exp(-400/T)$	20
44	$HCl + O \rightarrow OH + Cl$	$1.9\times10^{-11}\ \exp(-3573/T)$	21
45	$Cl + CH_4 \rightarrow HCl + CH_3$	$5.1\times10^{-11}\ \exp(-1790/T)$	21
46	$Cl + H_2 \rightarrow HCl + H$	$2.0\times10^{-11}\ \exp(-2164/T)$	21
47	$Cl + O_3 \rightarrow ClO + O_2$	$3.4\times10^{-11}\ \exp(-300/T)$	20
48	$ClO + O \rightarrow Cl + O_2$	5.7×10^{-11}	21
49	$ClO + NO \rightarrow NO_2 + Cl$	1.7×10^{-11}	21
50	$ClO + CO \rightarrow CO_2 + Cl$	1.7×10^{-15}	21

[a]Units in sec^{-1} for unimolecular reactions, $cm^3\ sec^{-1}$ for bimolecular reactions, $cm^6\ sec^{-1}$ for termolecular reactions.

[b]The pressure-dependent rate constant is calculated using a three-level system and is fitted to available rate data at high, low, and intermediate pressures. Details are given in Turco and Whitten.[17]

[c]Values are based on the measurement of the total reaction rate of O and H_2O_2 by Garvin and Hampson[18] and the ratio of the reaction rates for reactions 41 and 42 recommended by Nicolet.[19]

Transport

The mean meridional circulation is obtained by the kinematic method from the averaged equation of mass continuity. With the assumption that the density field is in a steady state, the approximate form of this equation in spherical coordinates is

$$\frac{1}{R\cos\phi}\frac{\partial(\bar{\rho}\bar{v}\cos\phi)}{\partial\phi}+\frac{\partial(\bar{\rho}\bar{w})}{\partial z}=0 \qquad (5)$$

where the overbar denotes an average with respect to time and longitude, $\bar{\rho}$ is the bulk density, $\bar{v}$ and $\bar{w}$ are the meridional and vertical velocity components, R is the radius of the earth, and ϕ the latitude. Equation (5) implies the existence of a except HNO_3, NO_2, O_3, N_2O, $HC\ell$, and H_2O_2 is chemical

Table 2 Photodissociation rates for O-H-N-Cl system (in units of sec^{-1} at zero optical depth)

Number	Process	Rate coefficient	Reference
J1	$O_2 + h\nu \rightarrow 2\ O(^3P)$	3.6×10^{-6}	22, 23, 24, 25
J2	$O_3 + h\nu \rightarrow O_2 + O(^3P)$	5.6×10^{-4}	26, 27, 28
J3	$O_3 + h\nu \rightarrow O_2 + O(^1D)$	9.6×10^{-3}	26, 27, 28
J4	$NO + h\nu \rightarrow N + O$	1.4×10^{-5}	29
J5	$NO_2 + h\nu \rightarrow NO + O$	1.0×10^{-2}	30, 31, 32
J6	$H_2O + h\nu \rightarrow OH + H$	5.6×10^{-6}	33
J7	$HNO_3 + h\nu \rightarrow NO_2 + OH$	1.4×10^{-4}	34, 35
J8	$HNO_2 + h\nu \rightarrow NO + OH$	6.6×10^{-4}	36
J9	$N_2O + h\nu \rightarrow N_2 + O(^1D)$	1.4×10^{-6}	37, 38, 39
J10	$NO_3 + h\nu \rightarrow NO_2 + O$	2.55×10^{-2}	36
	$\rightarrow NO + O_2$	4.08×10^{-2}	36
J11	$N_2O_5 + h\nu \rightarrow 2\ NO_2 + O$	6.0×10^{-4}	40
J12	$HO_2 + h\nu \rightarrow OH + O$	1.0×10^{-3}	41
J13	$H_2O_2 + h\nu \rightarrow 2\ OH$	1.7×10^{-4}	42, 43
J14	$HCl + h\nu \rightarrow H + Cl$	2.4×10^{-5}	44
J15	$ClO + h\nu \rightarrow O + Cl$	4.5×10^{-3}	45

"stream function" ψ for the total mass flux such that

$$2\pi R\bar{\rho}\bar{v}\cos\phi=-\frac{\partial\psi}{\partial z} \qquad 2\pi R\bar{\rho}\bar{w}\cos\phi=\frac{\partial\psi}{R\partial\phi} \qquad (6)$$

If the distrubution of $\bar{\rho}$ and $\bar{v}$ is known, the first of these can be integrated vertically, and $\bar{w}$ can be obtained from the second.

Up to 20 km, the density was obtained from data presented by Oort and Rasmusson,[46] and above that altitude by vertical integration of the hydrostatic equation, using mean (rocket) temperatures.[47]

The $\bar{v}$ components were based on the results[46] up to 20 km. These values were then extrapolated to the top of the model by imposition of a simple vertical profile that matched the 20-km value and satisfied the kinematic constraint that there be no equilibrium. Because HNO_3, $HC\ell$, and H_2O_2 are water soluble, their number densities are set equal to zero at the lower boundary. The number densities of NO_2 and N_2O are fixed at 3×10^9 cm^{-3} and $7.5\times10^{+12}$ cm^{-3}, respectively, at the lower boundary while that of O_3 is fixed at 6×10^{11} cm^{-3} (see Ref. 9).

The chemistry employed in this model is a simplified version of that used in our one-dimensional model studies.[10] At each time step, the model calculates the concentrations of O_3, $O(^3P)$, $O(^1D)$, NO_2, NO, NO_3, N_2O, N_2O_5, HNO_3, HNO_2, H_2O_2, HO_2, N, OH, H, $C\ell$, $C\ell O$, and $HC\ell$. The profiles of N_2, O_2, H_2O, H_2, CH_4, CO, and CO_2 are held fixed (at the experimentally determined values) during the calculations.

The rate coefficients are shown in Table 1, and the photolysis rates at zero optical depth are given in Table 2.

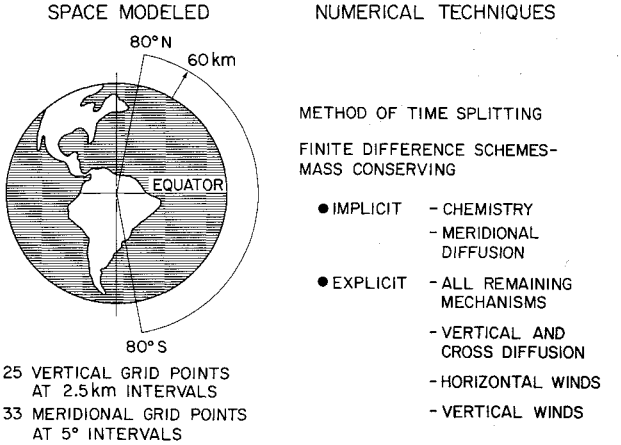

Fig. 1 Model geometry and techniques.

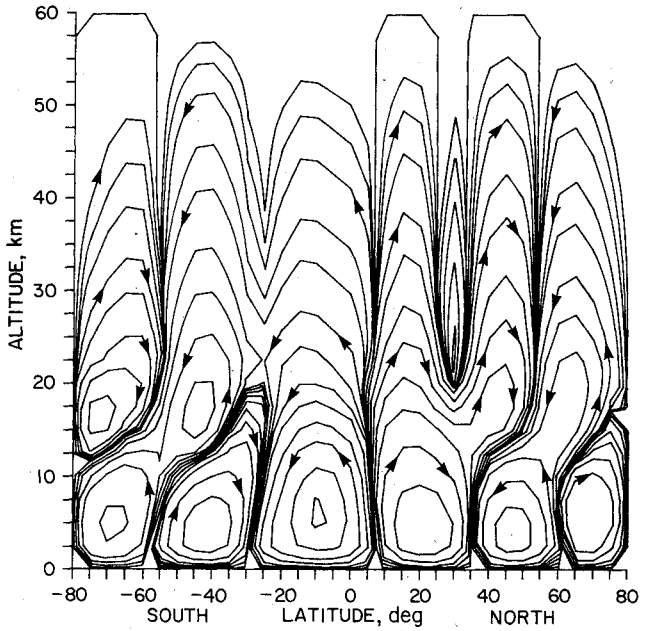

Fig. 2 Stream function; fall in the northern hemisphere.

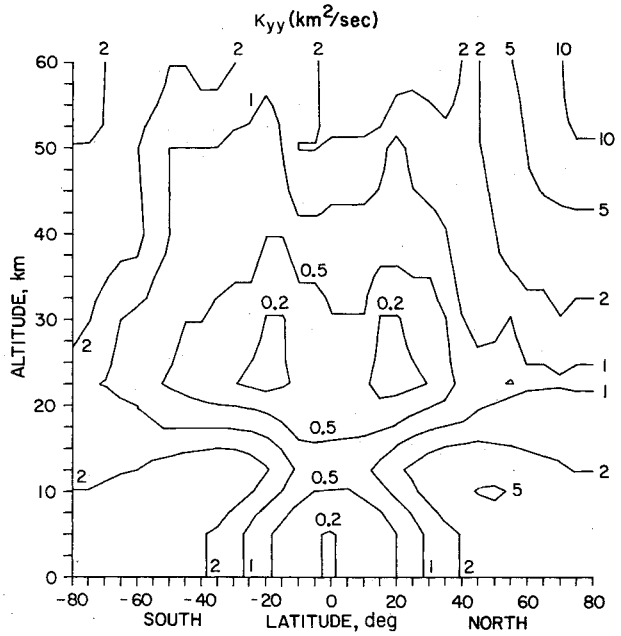

Fig. 3 K_{yy}; fall in the northern hemisphere.

net mass flux across any vertical latitude wall. This constraint arises because the model has a rigid top and bottom. In addition, a meridional variation was imposed that resulted in a three-cell circulation structure (80°N–80°S) in the stratosphere and lower mesosphere during the summer and winter seasons and four-cell structure in spring and fall. This should approximate the circulation patterns obtained by other investigators (e.g., Murgatroyd and Singleton,[48] Vincent[49]). The first segment of Eq. (6) was then integrated vertically with the condition that $\psi = 0$ on all boundaries. The resulting circulation patterns are reasonable in the troposphere and lower stratosphere (Fig. 2) but need further refinement in the upper portion of the model.

There are always uncertainties in the mean meridional circulation, even in the troposphere where sufficient wind data are available. Meridional wind speeds are generally less than 1 m/sec, except in the upper equatorial troposphere. Vertical wind speeds attain maxima in excess of 4 mm/sec in the equatorial troposphere; but are usually less than 1 mm/sec except in the vicintiy of cell boundaries.

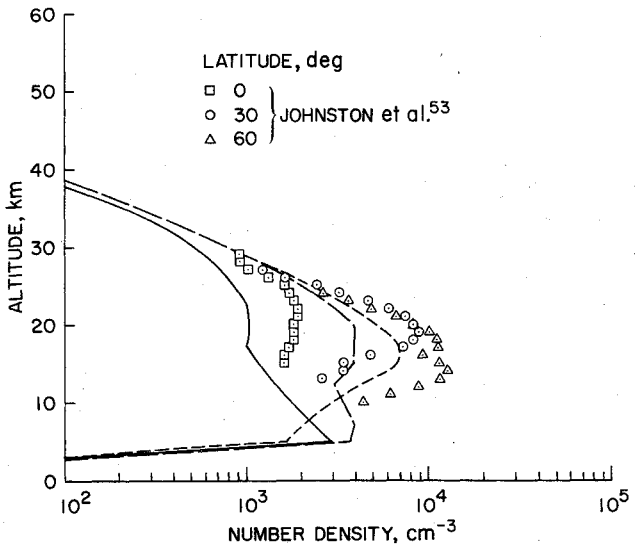

Fig. 4 Vertical distributions of carbon 14 at various latitudes. Experimental points are from Johnston et al.[53]

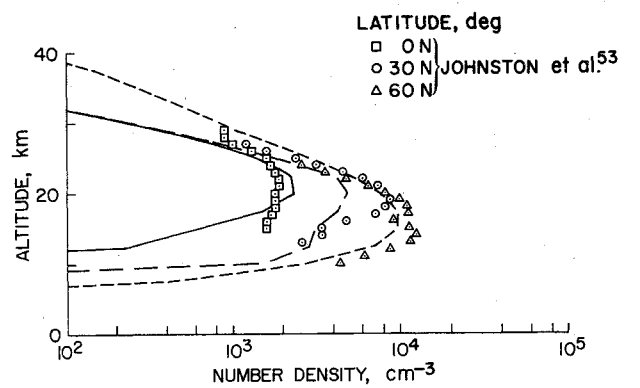

Fig. 5 Calculated vs predicted carbon 14 concentrations for the adjusted winds and transport coefficients of Louis.[54]

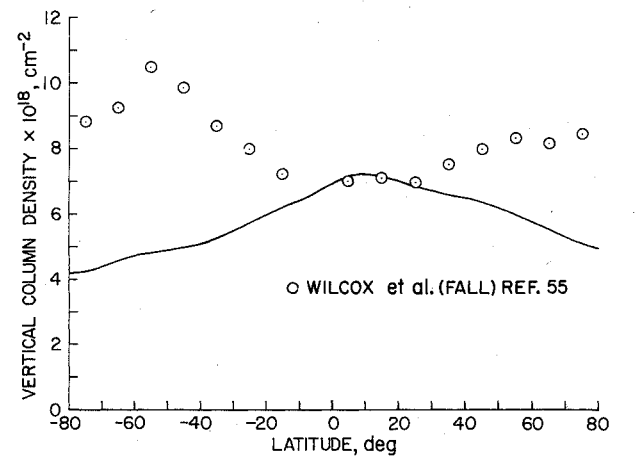

Fig. 6 Calculated vs predicted ozone column density as a function of latitude for the adjusted winds and transport coefficients of Louis.[54]

The eddy fluxes are modeled by diffusion coefficients based on the method of Reed and German.[50] The data of Luther[51] were used up to 20 km. These values were extended to the higher levels by assuming that K_{yy} is proportional to the variance of the v component, and that the slopes of the mixing surfaces are proportional to the slopes of the mean isentropic surfaces. Given K_{yy}, the other coefficients were obtained from (see Reed and German[50])

$$K_{yz} = \tilde{\alpha} K_{yy} \qquad K_{zz} = (\tilde{\alpha}^2 + \overline{\alpha'^2}) K_{yy} \tag{7}$$

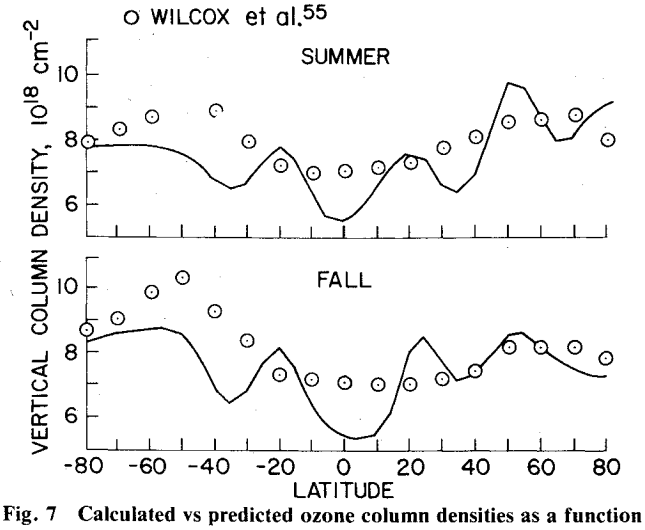

Fig. 7 Calculated vs predicted ozone column densities as a function of latitude for two seasons. The measurements were taken from Wilcox et al.[55]

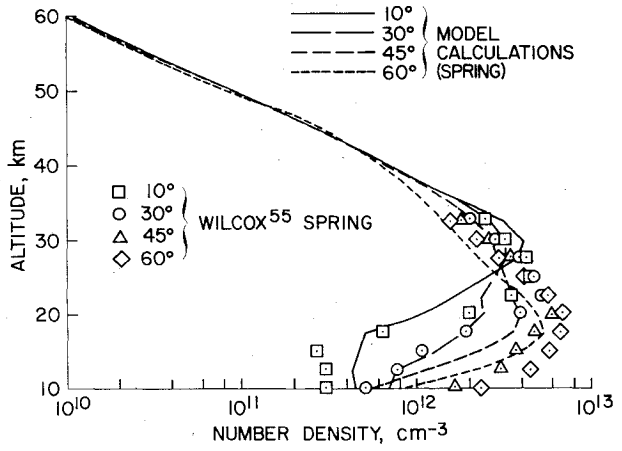

Fig. 8 Calculated vs predicted ozone concentration as a function of altitude for four different latitudes. Measurements are those of Wilcox et al.[55]

where $\bar{\alpha}$ is the mean slope of the mixing surface, and $\overline{\alpha'^2}$ its variance. The value of $\overline{\alpha'^2}$ was assumed to be constant. The variances of v were taken from Nastrom et al.[52] Representative K_{yy} values are shown in Fig. 3.

Results

Using the model described in the preceding sections, we have computed the spread of an inert radioactive tracer (carbon 14) from the 1963–1965 nuclear-test data presented by Johnston et al.[53] The model was started by using the Jan. 1963 data for the initial number densities and run for 1 year (i.e., 4 seasons). The results are presented as lines appropriate for 0°, 30°, and 60°N latitudes. The data points shown on Fig. 4 are the measured carbon 14 concentrations vs altitude for three latitudes for Jan. 1964. This figure shows that, although the calculated number densities follow the shape of the measured curves above 10 km, they are generally too low, sometimes by a factor of two. This implies that the calculated loss rate of the tracer is larger than observed and that calculations using the transport previously described tend to underestimate the residence time of any injected species.

Unfortunately, it is not sufficient to simply pick a set of seasonal winds and transport coefficients that result in a good prediction for the disappearance of carbon 14 with time. Figure 5 compares the predicted and measured carbon 14 concentrations when the transport coefficients of Louis[54] were

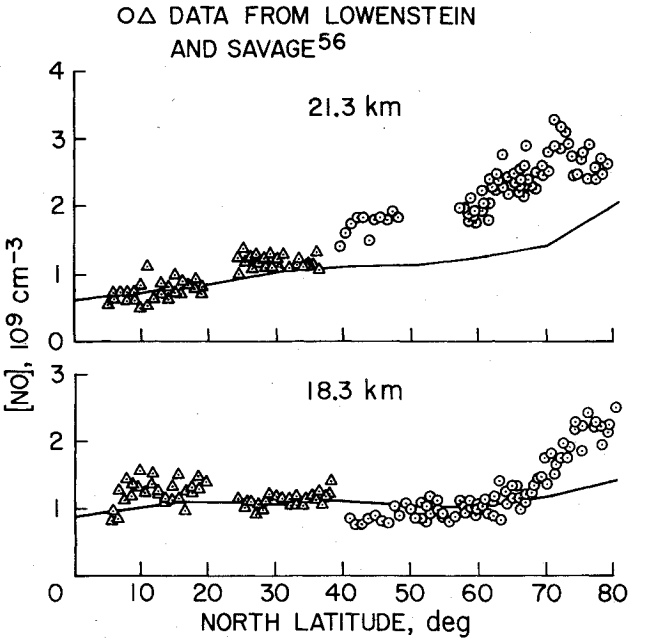

Fig. 9 Nitric oxide number densities vs latitude for two altitudes. The symbols represent the measurements of Loewenstein and Savage.[56] Both the data and calculations are for local noon of a summer season.

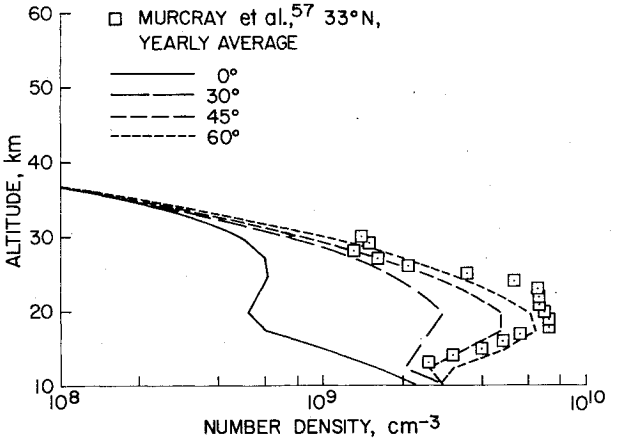

Fig. 10 Calculated vs measured nitric acid (HNO_3) concentration as a function of altitude for four different latitudes. Data are taken from the work of Murcray et al.[57]

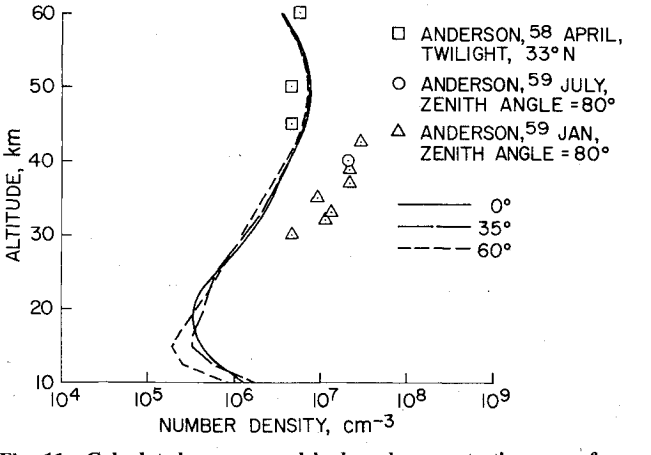

Fig. 11 Calculated vs measured hydroxyl concentrations as a function of altitude for four different latitudes. The measurements are taken from Anderson.[58,59]

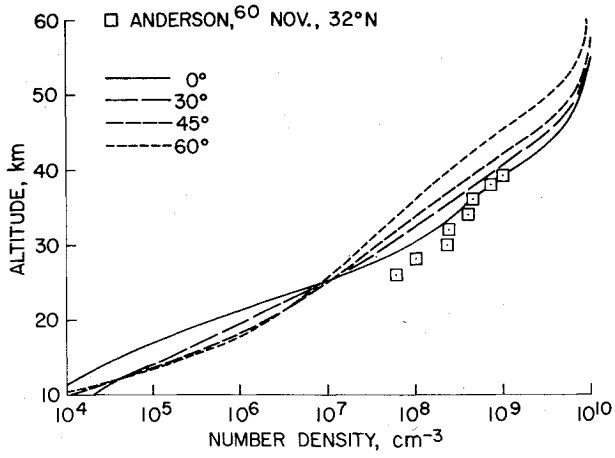

Fig. 12 Calculated vs measured atomic oxygen concentrations as a function of altitude for four different latitudes. The measurements are from Anderson.[60] The calculations for for local noon in the Winter season.

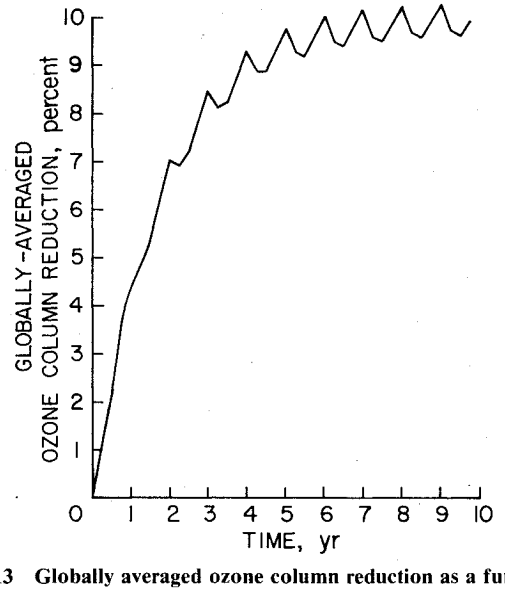

Fig. 13 Globally averaged ozone column reduction as a function of time after initiation of hypothetical SST operations.

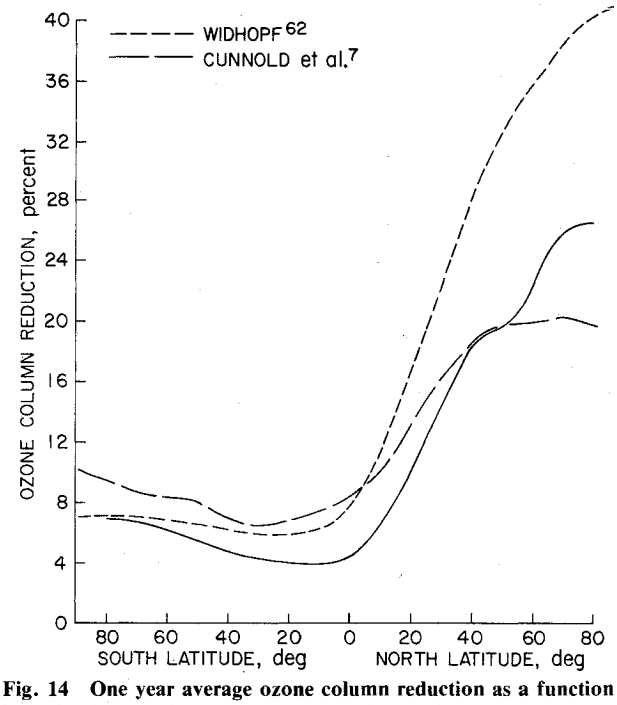

Fig. 14 One year average ozone column reduction as a function of latitude 10 years after commencement of operations.

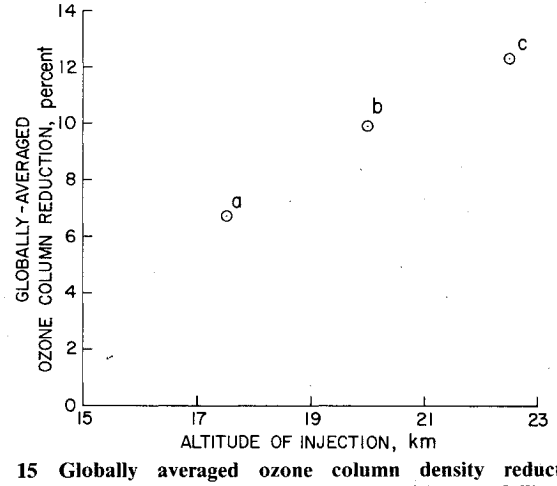

Fig. 15 Globally averaged ozone column density reduction following 10 years of SST operations at three altitudes of flight: a) 17.5 km, b) 20 km, and c) 22.5 km.

used with his wind velocities reduced by a factor of three. However, when these transport coefficients and reduced wind velocities were used to calculate the ozone and other trace species distributions, the ozone distribution was in strong disagreement with the measurements (see Fig. 6). Much better agreement between the measured and predicted ozone distribution is obtained when the unmodified winds and transport coefficients described previously are used (see Fig. 7). This figure shows that the absolute level of ozone is about right and that the predicted value oscillates about the measurements. The local maxima and minima in the predicted curve are evidently due to the use of a set of transport coefficients that is independent of the winds chosen. Hence, the following results must be considered preliminary pending further improvement of the transport parameters.

It should be emphasized here that all of the following results, and those shown in Fig. 7, are based on the winds and transport coefficients described in the section titled "Transport" and are not those of Louis.[54]

The program was run to simulate a period of 10 years, which was sufficient to approach a steady state. Figures 8-12 show the calculated number of densities of O_3, NO, HNO_3, OH, and $O(^3P)$ vs altitude for the ambient atmosphere. An examination of the figures shows that our predictions agree reasonably well with the measurements where these are available. Variations of species concentrations with both latitude and season are evident. Having thus demonstrated that the model predicts reasonably well the concentrations of a number of species in the unperturbed stratosphere, we can now investigate some of the effects of aerospace vehicle operations in the stratosphere.

To calculate the perturbation of stratospheric ozone caused by a fleet of SSTs, two computer runs were made: one for the ambient atmosphere and a second run identical to the first except that NO_2 was injected at a rate of 1.8×10^6 metric tons** per year at an altitude of 20 km for latitudes between 40° and 50°N.

The calculated reduction in global ozone due to NO_2 injection from a future fleet of supersonic transports vs time is given in Fig. 13. After a 10-year integration time, the reduction has reached 10%. Figure 14 displays the reduction as a function of latitude. The dashed curve in Fig. 14 represents

**This injection rate is equal to that used by Cunnold et al.[7] in their calculations. It represents approximately 1000 advanced SSTs operating 7 hr per day.

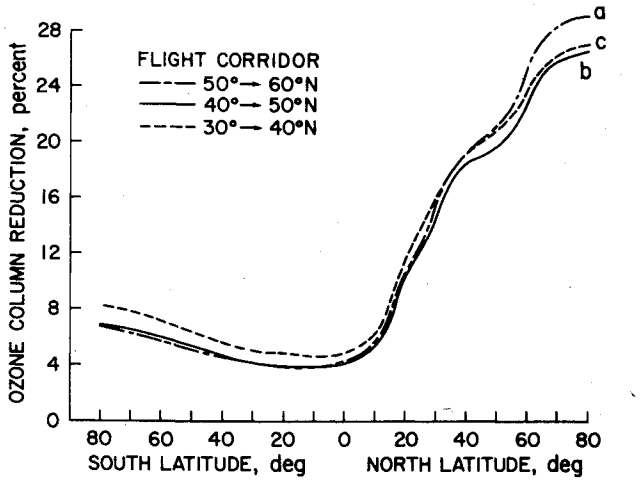

Fig. 16 Calculated ozone column density reductions as a function of latitude for three different flight corridors: a) 50°N-60°N, b) 40°N-50°N, c) 30°N-40°N.

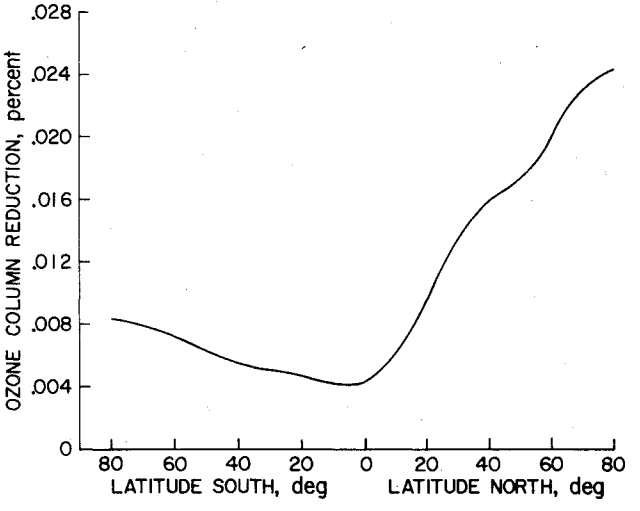

Fig. 17 Calculated ozone column density reduction vs latitude for the Concorde flight schedule listed in Table 3.

the results of a three-dimensional model run from Cunnold et al.[7] for a similar episode of injection. It can be seen from Fig. 14 that our model predicts a latitude-dependent ozone depletion similar in appearance to that given by Cunnold et al.[7] They report a globally averaged ozone depletion of 12% in good agreement with our model prediction of 10% for the same flight frequency and altitude. The results of Widhopf[62] are also shown in Fig. 14. Their results for the Northern Hemisphere are much higher than those of the Ames two-dimensional model and those of Cunnold et al.[7] This difference might be due to their use of winds and transport coefficients that do not vary seasonally. Nevertheless, all three sets of calculations indicate a strong corridor effect in that the predicted ozone depletions are largest to the north of the flight corridor for aircraft operating in the northern hemisphere.

We have also tested the sensitivity of the ozone depletion with respect to SST flights at different altitudes and flight corridors. Figure 15 shows the globally averaged ozone depletion for three different altitudes of flight for 10 years of simulated operations. Clearly our model predicts increased ozone depletions at higher flight altitudes. In Fig. 16 we show the effects due to different flight corridors. It can be seen that the latitude dependence of the ozone column depletion is relatively insensitive to the flight corridors chosen in this simulation.

Table 3 Flight schedule and emission characteristics for the British-French Concorde[61]

Flight schedule:	
London 52° N, 0° to Bahrein 25° N, 52° E	4/week
London 52° N, 0° to New York 41° N, 74° W	14/week
Paris 49° N, 2-1/2° E to New York 41° N, 74° W	14/week
London 52° N, 0° to Washington 38° N, 77-1/2° W	14/week
Paris 49° N, 2-1/2° E to Washington 38° N, 77-1/2° W	14/week
Paris 49° N, 2-1/2° E to Rio 21° S, 41° W	2/week
Bahrein 25° N, 52° E to Singapore 2° N, 104° E	3/week
Singapore 2° N, 104° E to Melbourne 38° S, 145° E	3/week
Emission characteristics:	
Speed	2130 km/hr
Altitude	15 km first 2/3 of flight 17-1/2 km last 1/3 of flight
NO_2 emission	340 kg/hr NO_2

We stress here that the previous discussion regarding the effects of SST operations in the stratosphere is appropriate for the standard problem of 1000 supersonic transports operating 7 hr per day. A fleet of such magnitude is not anticipated in the near future. A more realistic assessment of the potential effects of SST operations on stratospheric ozone can be obtained by considering the current British-French Concorde flight schedule. Assuming the flight emmission characteristics given in Table 3, we have again run our model as described above to simulate a period of 10 years. A careful comparison of Figs. 16 and 17 shows that there is *relatively* more ozone reduction in the Southern Hemisphere than in the Northern Hemisphere for the Concorde case. This is to be expected because the Concorde flight schedule calls for flights in the Southern Hemisphere as well as in the Northern Hemisphere. The globally averaged ozone reduction was then found to be 0.01%, a value three decades lower than that obtained from the hypothetical fleet of 1000 flights/day. However, before we can regard our estimates as definitive, the transport of trace species in the atmosphere must be better understood and documented, and the model modified accordingly.

References

[1] Johnston, H. S., "Reduction of Stratospheric Ozone by Nitrogen Oxide Catalysts from Supersonic Transport Exhaust," *Science,* Vol. 173, 1971, p. 517.

[2] McElroy, M. B., Wofsy, S. C., Penner, J. E., and McConnell, J. C., "Atmospheric Ozone: Possible Impact of Stratospheric Aviation," *Journal of the Atmospheric Sciences,* Vol. 31, 1974, p. 287.

[3] Crutzen, P. J., "SST's: A Threat to the Earth's Ozone Shield," *Ambio,* Vol. 1, 1972, p. 41.

[4] Whitten, R. C., Borucki, W. J., and Turco, R. P., "One-Dimensional-Model Studies of Ozone Depletion," *Proceedings of the Third Conference on the Climatic Impact Assessment Program,* DOT-TSC-OST-74-15, 1974, p. 342, Dept. of Transportation, Washington, D. C.

[5] Widhopf, G. F. and Taylor, T. D., "Numerical Experiments on Stratospheric Meridional Ozone Distributions Using a Parameterized Two-Dimensional Model," *Proceedings of the Third Conference on the Climatic Immpact Assessment Program,* DOT-TSC-OST-74-15, 1974, p. 376, Dept. of Transportation, Washington, D. C.

[6] Shimazaki, T., Wuebbles, D. J., and Ogawa, T., "A Two-Dimensional Theoretical Model for Stratospheric Ozone Density Distributions in the Meridional Plane," ERL-279-OD-9, 1973, National Oceanic and Atmospheric Administration, Washington, D. C.

[7] Cunnold, D. M., Alyea, F. N., Phillips, N. A., and Prinn, R. G., "First Results of a General Circulation Model Applied to the SST-NO_x Problem," *Second International Conference on the Environmental Impact of Aerospace Operations in the High Atmosphere,* American Meteorological Society, San Diego, Calif., July 1974, p. 187.

[8]Hesstvedt, E., "Reduction of Stratospheric Ozone from High-flying Aircraft, Studied in a Two-dimensional Photochemical Model with Transport," *Canadian Journal of Chemistry,* Vol. 52, 1974, p. 1592.

[9]Wu, Mao-Fu, "Trace Constituents in the Stratosphere," Annual Report ERT-0393, July 1974, Dept. of Transportation, Washington, D. C.

[10]Whitten, R. C. and Turco, R. P., "Perturbations of the Stratosphere and Mesosphere by Aerospace Vehicles," *AIAA Journal,* Vol. 12, Aug. 1974, pp. 1110-1117.

[11]Garvin, D., ed., "Chemical Kinetics Data Survey IV," NBSIR-203, 1973, National Bureau of Standards, Washington, D. C.

[12]Hampson, R. F. and Garvin D., "Chemical Kinetics and Photochemical Data for Modelling Atmospheric Chemistry," NBS Technical Note 866, 1975, National Bureau of Standards, Washington, D. C.

[13]Davis, D. D., Herron, J. T., and Huie, R. E., "Absolute Rate Constants for the Reaction $O(^3P)+NO_2 \rightarrow NO+O_2$ Over the Temperature Range 230-339 K," *Journal of Chemical Physics,* Vol. 58, 1973, p. 530.

[14]Hampson, R. F., ed., "Chemical Kinetics Data Survey I," NBS Rept. 10692, National Bureau of Standards, Washington, D. C.

[15]Young, R. A. and Sharples, R. H., "Chemiluminescent Reactions Involving Atomic Oxygen and Nitrogen," *Journal of Chemical Physics,* Vol. 39, 1963, p. 1071.

[16]Baulch, D. L., Drysdale, D. D., and Horne, D. G., *Evaluated Kinetics Data for High Temperature Reactions,* Vol. 3, CRC Press, Cleveland, Ohio, 1973.

[17]Turco, R. P. and Whitten, R. C., "Chlorofluoromethanes in the Stratosphere and Some Possible Consequences for Ozone," *Atmospheric Environment,* Vol. 9, 1975, p. 1045.

[18]Garvin, D. and Hampson, R. F., eds., "Chemical Kinetics Data Survey VII," Rept. NBSIR 74-430, 1974, National Bureau of Standards, Washington, D. C.

[19]Nicolet, Marcel, "Aeronomic Chemistry of the Stratosphere," *Planetary and Space Science,* Vol. 20, 1971, p. 1671.

[20]Watson, R. T., "Chemical Kinetics Data Survey VIII," NBSIR 74-576, 1974, National Bureau of Standards, Washington, D. C.

[21]Watson, R. T. personal communication, 1975.

[22]Hudson, R. C. and Mahle, S. H., "Photodissociation Rates of Molecular Oxygen in the Mesosphere and Lower Thermosphere," *Journal of Geophysical Research,* Vol. 77, 1972, p. 2902.

[23]Ogawa, M., "Absorption Coefficients of O_2 at the Lyman-α Line and Its Vicinity," *Journal of Geophysical Research,* Vol. 73, 1968, p. 6759.

[24]Blake, A. J., Carver, J. H., and Haddad, G. N., "Absorption Cross Sections of Molecular Oxygen Between 1250 Å and 2350 Å," *Journal of Quantitative Spectroscopy and Radiative Transfer,* Vol. 6, 1966, p. 451.

[25]Watanabe, K., Inn, E. C. Y., and Zelikoff, M., "Absorption Coefficients of Oxygen in the Vacuum Ultraviolet," *Journal of Chemical Physics,* Vol. 21, 1953, p. 1026.

[26]Inn, E. C. Y. and Tanaka, Y., "Absorption Coefficient of Ozone in the Ultraviolet and Visible Regions," *Journal of the American Optical Society,* Vol. 43, 1953, p. 870.

[27]Griggs, M., "Absorption Coefficients of Ozone in the Ultraviolet and Visible Regions," *Journal of Chemical Physics,* Vol. 49, 1968, p. 857.

[28]Jones, I. T. N. and Wayne, R. P., "Photolysis of Ozone by 254-, 313-, and 334-nm Radiation," *Journal of Chemical Physics,* Vol. 51, 1969, p. 3617.

[29]Cieslik, S. and Nicolet, M., "The Aeronomic Dissociation of Nitric Oxide," *Planetary and Space Science,* Vol. 21, 1973, p. 925.

[30]Hall, T. C. and Blacet, F. E., "Separation of the Absorption Spectra of NO_2 and N_2O_4 in the Range of 2400-5000 Å," *Journal of Chemical Physics,* Vol. 20, 1952, p. 1745.

[31]Nakayama, T., Kitamura, M. Y., and Watanabe, K., "Ionization Potential and Absorption Coefficients of Nitrogen Dioxide," *Journal of Chemical Physics,* Vol. 30, 1959, p. 1180.

[32]Pitts, J. N., Sharp, J. H., and Chan, S. I., "Effects of Wavelength and Temperature on Primary Processes in the Photolysis of Nitrogen Dioxide and a Spectroscopic-Photochemical Determination of the Dissociation Energy," *Journal of Chemical Physics,* Vol. 40, 1964, p. 3655.

[33]Watanabe, K. and Zelikoff, M., "Absorption Coefficients of Water Vapor in the Vacuum Ultraviolet," *Journal of the American Optical Society,* Vol. 43, 1953, p. 753.

[34]Johnston, H. S. and Graham, R., "Gas-Phase Ultraviolet Absorption Spectrum of Nitric Acid Vapor," *Canadian Journal of Chemistry,* Vol. 52, 1974, p. 8.

[35]Johnston, H. S., *CIAP Newsletter,* Vol. 72-4, 1972, Dept. of Transportation, Washington, D. C.

[36]Johnston, H. S., and Graham, R., "Photochemistry of NO_x and HNO_x Compounds," *Journal of Physical Chemistry,* Vol. 77, 1972, p. 62.

[37]Zelikoff, M., Watanabe, K., and Inn, E. C. Y., "Absorption Coefficients in Gases in the Vacuum Ultraviolet. Part II. Nitrous Oxide," *Journal of Chemical Physics,* Vol. 21, 1953, p. 1643.

[38]Bates, D. R. and Hays, P. B., "Atmospheric Nitrous Oxide," *Planetary and Space Science,* Vol. 15, 1967, p. 189.

[39]Preston, K. F. and Barr, R. F., "Primary Processes in the Photolysis of Nitrous Oxide," *Journal of Chemical Physics,* Vol. 54, 1971, p. 3347.

[40]Jones, E. J. and Wulf, O. R., "The Absorption Coefficient of Nitrogen Pentoxide in the Ultraviolet and Visible Absorption Spectrum of NO_3," *Journal of Chemical Physics,* Vol. 5, 1937, p. 873.

[41]Paukert, T. T. and Johnston, H. S., "Spectra and Kinetics of the Hydroperoxyl Free Radical in the Gas Phase," *Journal of Chemical Physics,* Vol. 56, 1973, p. 2824.

[42]Urey, H. C., Dawsey, L. H., and Rice, F. O., "The Absorption Spectrum and Decomposition of Hydrogen Peroxide by Light," *Journal of the American Chemical Society,* Vol. 51, 1929, p. 1371.

[43]Holt, R. B., McLane, C. K., and Oldenberg, O., "Ultraviolet Absorption Spectrum of Hydrogen Peroxide," *Journal of Chemical Physics,* Vol. 16, 1948, p. 225.

[44]Myer, J. A. and Samson, J. A. W., "Vacuum-Ultraviolet Absorption Cross Sections of CO, HCℓ, and ICN between 1050 and 2100 Å," *Journal of Chemical Physics,* Vol. 52, 1970, p. 266.

[45]Johnston, H. S., Morris, E. D., and Van de Bogaer, "Molecular Modulation Kinetic Spectrometry, CLOO and CLO_2 Radicals in the Photolysis of Chlorine in Oxygen," *Journal of the American Chemical Society,* Vol. 91, 1969, p. 7712.

[46]Oort, A. H. and Rasmussen, E. M., "Atmospheric Circulation Statistics," NOAA Professional Paper 5, 1971, National Oceanic and Atmospheric Administration, Washington, D. C.

[47]Nastrom, G. D. and Belmont, A. D., "Diurnal Stratospheric Tide in Meridional Wind, 30 to 60 km, by Season and Monthly Mean Temperatures, 20 to 60 km, at 80°N to 0°N," CR137738, 1975, NASA.

[48]Murgatroyd, R. J. and Singleton, F., "Possible Meridional Circulations in the Stratosphere and Mesosphere," *Quarterly Journal of the Royal Meteorological Society,* Vol. 87, 1961., pp. 125-135.

[49]Vincent, D. G., "Mean Meridional Circulations in the Northern Hemisphere Lower Stratosphere During 1964, and 1965," *Quarterly Journal of the Royal Meteorological Society,* Vol. 94, 1968, pp. 333-349.

[50]Reed, R. J. and German, K. E., "A Contribution to the Problem of Stratospheric Diffusion by Large-Scale Mixing," *Monthly Weather Review,* Vol. 93, 1965, p. 313.

[51]Luther, F. M., "Monthly Mean Values of Eddy Diffusion Coefficients in the Lower Stratosphere," AIAA Paper No. 73-498, AIAA/AMS International Conference on the Environmental Impact of Aerospace Operations in the High Atmosphere, Denver, Colo., June 1973.

[52]Nastrom, G. D., Belmont, A. D., and Dart, D. G., "Periodic Variations in Stratospheric Meridional Wind from 20-65 km at 80°N to 70°S," *Quarterly, Journal of the Royal Meteorological Society,* Vol. 101, 1975, pp. 583-596.

[53]Johnston, H. S., Kattenhorn, D., and Whitten, G., "Use of Excess Carbon 14 Data to Calibrate Models of Stratospheric Ozone Depletion by Supersonic Transports," *Journal of Geophysical Research,* Vol. 81, 1976, p. 368.

[54]Louis, Jean-Francois, "A Two-Dimensional Transport Model of the Atmosphere ," Ph.D. thesis, 1974, University of Colorado, Boulder, Colo.

[55]Wilcox, R. W., Nastrom, G. D., and Belmont, A. D., "Periodic Analysis of Ozone Variations, NASA, CR137737, 1975.

[56]Loewenstein, M. and Savage, H., "Latitudinal Measurements of NO and O_3 in the Lower Stratosphere from 5° to 82° North," *Geophysical Research Letters,* Vol. 2, 1975, p. 448.

[57]Murcray, D. G., Goldman, A., Williams, W. J., Murcray, F. H., Brooks, J. N., Van Allen, J., Stocker, R. N., Kosters, J. J., Barker, D. B., and Shider, D. F., "Recent Results of Stratosperic Trace-Gas Measurements from Balloon-Borne Spectrometers," *Proceedings of the Third Conference of the Climatic Impact Assessment Program,* Feb. 1974, p. 184, Dept. of Transportation, Washington, D.C.

[58]Anderson, J. G., "Rocket Measurement of OH in the Mesosphere," *Journal of Geophysical Research,* Vol. 76, 1971, p. 7820.

[59] Anderson, J. G., "The Absolute Concentration of OH($X^2\pi$) in the Earth's Stratosphere," *Geophysical Research Letters*, Vol. 3, 1976, pp. 165-168.

[60] Anderson, J. G., "The Absolute Concentration of O(^{3}P) in the Earth's Stratosphere," *Geophysical Research Letters*, Vol. 2, 1975, p. 231.

[61] Beadle, P., private communication, 1976.

[62] Widhopf, G.F., "Meridional Distribution of Trace Species in the Stratosphere and the Effect of SST Pollutants," presented at the American Geophysical Union Fall Annual Meeting, San Francisco, Calif., Sept. 1974.